# Effects of Model Resolution and Coverage on Storm-Driven Coastal Flooding Predictions

Ajimon Thomas[1]; J. C. Dietrich, M.ASCE [2]; C. N. Dawson[3]; and R. A. Luettich[4]

**Abstract:** Predictions of storm surge and flooding require models with higher resolution of coastal regions, to describe fine-scale bathymetric and topographic variations, natural and artificial channels, flow features, and barriers. However, models for real-time forecasting often use a lower resolution to improve efficiency. There is a need to understand how resolution of inland regions can translate to predictive accuracy, but previous studies have not considered differences between models that both represent conveyance into floodplains and are intended to be used in real time. In this study, the effects of model resolution and coverage are explored using comparisons between forecast-ready and production-grade models that both represent floodplains along the US southeast coast, but with typical resolutions in coastal regions of 400 and 50 m, respectively. For two storms that impacted the US southeast coast, it is shown that, although the overall error statistics are similar between simulations on the two meshes, the production-grade model allowed a greater conveyance into inland regions, which improved the tide and surge signals in small channels and increased the inundation volumes between 40% and 60%. Its extended coverage also removed water level errors of 20–40 cm associated with boundary effects in smaller regional models. **DOI: 10.1061/(ASCE) WW.1943-5460.0000687**.

## Introduction

There has always been a delicate balance between resolution and efficiency in coastal ocean circulation models that use unstructured meshes. Higher levels of resolution are required to represent: steep gradients in bathymetry, such as the continental shelf break (Westerink et al. 1992; Luettich and Westerink 1995; Blain et al. 1998; Hagen et al. 2000); wave propagation in shallow water regions (Hagen et al. 2001); and complex topography in overland regions (Westerink et al. 2008). Recent state-of-the-art meshes contain millions of triangular elements with sizes typically ranging from 4 to 6 km in the deeper ocean, from 500 to 1,000 m on the continental shelf, around 200 m within the coastal floodplains, and downward to 10 to 20 m within the fine-scale natural and artificial channels and barriers (Dietrich et al. 2011; Hope et al. 2013; Roberts et al. 2019). These "production-grade" meshes allow for accurate predictions of storm surge and coastal flooding, e.g., by the Federal Emergency Management Agency (FEMA) for flood risk mapping for the next generation of flood insurance rate maps (FIRMs) (Blanton and Luettich 2008; URS Corporation 2009; Bender 2013, 2014, 2015).

[1]Senior Scientist, Aon, 200 E Randolph St., Chicago, IL 60601. Email: athomas9@ncsu.edu

[2]Associate Professor, Dept. of Civil, Construction, and Environmental Engineering, North Carolina State Univ., 915 Partners Way, Raleigh, NC 27695 (corresponding author). ORCID: https://orcid.org/0000-0001-5294-2874. Email: jcdietrich@ncsu.edu

[3]Professor, Oden Institute for Computational Engineering and Sciences, Univ. of Texas at Austin, 201 E 24th St., Austin, TX 78712. ORCID: https://orcid.org/0000-0001-7273-0684. Email: clint@oden.utexas.edu

[4]Professor, Institute of Marine Sciences, Univ. of North Carolina, 150 Coker Hall, 3431 Arendell St., Morehead City, NC 28557. ORCID: https://orcid.org/0000-0002-7625-1952. Email: rick_luettich@unc.edu

Note. This manuscript was submitted on February 10, 2021; approved on August 20, 2021; published online on November 9, 2021. Discussion period open until April 9, 2022; separate discussions must be submitted for individual papers. This paper is part of the ***Journal of Waterway, Port, Coastal, and Ocean Engineering***, © ASCE, ISSN 0733-950X.

However, simulating several days of a storm on these state-of-the-art meshes can require several hours, even on thousands of computational cores (Tanaka et al. 2011; Roberts et al. 2021). This is costly, especially during forecasting applications where predictions are needed quickly. Therefore, current practice is to have "forecast-ready" meshes with sufficient resolution to provide fairly accurate predictions, while having considerably faster simulation time. An example is the Hurricane Surge On-Demand Forecast System (HSOFS) mesh (Riverside Technology and AECOM 2015), which was developed for tide and surge predictions for the entire US east coast from Texas to Maine. To reduce its computational cost, the average resolution along the shoreline was limited to about 500 m, which is much less than that of production-grade meshes. The HSOFS mesh has been used for real-time forecasting for extratropical storms by the National Oceanic and Atmospheric Adminstration (NOAA) and for tropical cyclones by academic researchers (CERA 2021).

Thus, there is a gap between forecast-ready meshes that aim to represent coastal floodplains with "medium" levels of resolution and production-grade meshes with the highest-possible levels of resolution. To bridge this gap, an emerging technology allows the use of high-resolution meshes only when and where required (Thomas et al. 2021). When the storm is far away from the coast, the simulation can start on a mesh with a relatively coarse representation of the coastline; then, when the storm approaches the coast, the simulation can be switched to a mesh with extensive detail in the projected landfall region. With this mesh-switching technique, preliminary results have shown efficiency gains of up to 53%, while retaining the accuracy of flooding predictions as compared with a full simulation on the higher-resolution mesh (Thomas et al. 2021). This new technique will expand the use of production-grade meshes in real-time forecasting. But there is a need to understand how their higher resolution may translate into higher accuracy.

Sensitivity to mesh resolution has been explored for predictions of tides and storm surge, but not for forecasting. For simulations of tides in the South Atlantic Bight (SAB), tests with varying geometries indicated that the inclusion of tidal inlets, artificial channels, estuaries, and marshes can improve model skill, increase the tidal

amplitude by 5%–10% on the shelf (Blanton et al. 2004), and modify the tidal propagation and resonance (Bacopoulos and Hagen 2017). For simulations of storm surge and coastal flooding, the benefits of higher resolution have typically been demonstrated as an improvement over previous studies, e.g., the increased accuracy for simulations with progressively higher resolution in southeast Louisiana (Westerink et al. 2008; Bunya et al. 2010; Dietrich et al. 2011). It has been relatively rare for these benefits to be examined within the same study, especially for a real coastal region. For simulations of Hurricane Ike (September 2008) in Texas and Louisiana (Kerr et al. 2013), higher mesh resolution was shown to enable surge propagation and attenuation in inland water bodies and overland. For simulations of storms along the US Atlantic coast (Lawler et al. 2016), higher mesh resolution was also shown to enable flow connectivity to remote locations and improve the predictions. However, in these comparisons, the "coarse" meshes were too coarse, so that many flow pathways and barriers were not represented, and thus the findings were binary, in that they indicated that it is better to include a coastal feature than not. There is still a need to quantify the benefits of varying resolution and representing features in both forecast-ready and production-grade meshes.

The goal of this study is to better understand the role of resolution and coverage of unstructured meshes on predictions of water levels, with a motivation for real-time forecasting. It is hypothesized that a new production-grade mesh, with higher-resolution capabilities and with coverage all along the US southeast coast, will increase accuracy of flooding predictions relative to a forecast-ready mesh. This hypothesis is evaluated by (a) developing a higher-resolution mesh with detailed coverage of the floodplains from Florida through North Carolina, (b) validating model predictions of water levels during two storms that impacted the US southeast coast in different ways, (c) quantifying the gain in accuracy of flooding predictions over those from a forecast-ready mesh, and (d) quantifying the role of mesh-coverage on predictions by comparisons of maximum water levels with those from single simulations on two regional meshes.

## Methods

In this study, a higher-resolution mesh for the floodplains along the SAB is developed by combining five regional meshes with an open-water mesh. In this section, we describe the regional meshes, the process of mesh development, the wind and pressure fields used as model forcing, the simulation settings, and how the results were analyzed.

### *SAB Mesh Development*

#### Regional Meshes

The five regional meshes were created for FEMA flood insurance studies (FISs) in North Carolina (NC), South Carolina (SC), Georgia and Northeast Florida (GANEFL), East Coast Central Florida (ECCFL), and South Florida (SFL) (Blanton and Luettich 2008; URS Corporation 2009; Bender 2013, 2014, 2015). The details regarding these meshes are given in Table 1. Some of the meshes were provided in draft form and, with improvements by the study team, do not reflect the final mesh from an effective FIS. The final meshes for each regional study can be accessed through the FEMA Engineering Library (FEMA 2021). By using these five regional meshes, their previous development can be leveraged. Each mesh has been validated and tested; thus, it should already provide a good representation of its coastal regions and possible storm-driven flooding. These strengths can then be carried forward in the development of the SAB mesh.

**Table 1.** Details regarding the regional and large-domain meshes

| Mesh | Version | Vertices | Elements | Typical resolution (m) |
|---|---|---|---|---|
| NC9 | 9.99 | 624,782 | 1,234,231 | 100 |
| SC | 12 | 542,809 | 1,073,925 | 100 |
| GANEFL | 12 | 2,968,735 | 5,910,443 | 50–100 |
| ECCFL | 6 | 1,406,543 | 2,793,387 | 80–200 |
| SFL | 11 | 2,249,093 | 4,480,230 | 75 |
| HSOFS | 1e | 1,813,443 | 3,564,104 | 400 |
| SAB | 1 | 5,584,241 | 11,066,018 | 100 |

The North Carolina (NC9) mesh extends inland to the 15 m topographic contour to allow for storm surge flooding (Blanton and Luettich 2008). Mesh spacing along the NC coastline varies from 3–4 km on the continental shelf to about 100 m near the Outer Banks. The resolution goes below 50 m in the narrow river channels that extend inland from the sounds and elsewhere along the NC coastline (Cyriac et al. 2018). The SC mesh was built by combining a higher-resolution mesh of the SC coastal zone with a coarser large-domain model of the the western North Atlantic (Westerink et al. 1993; Scheffner and Carson 2001). The resolution varies from 2–3 km on the continental shelf to 100 m along the coast, including such regions as Charleston Harbor (WEC 2016; URS Corporation 2009). The SC mesh has the coarsest coastal resolution of all the component meshes. The GANEFL mesh was developed by combining a high-resolution mesh of the region with the coarser EC2001 mesh (Mukai et al. 2002). The mesh has an element spacing of 50–100 m along the coastline, with the spacing going down to 25–30 m in the smaller channels (Bender 2013; Naimaster et al. 2013). Element sizes of 80 to 200 m extend 4.8 km offshore, with a 4 km resolution at the eastern shelf edge. The ECCFL mesh was developed with a goal to determine the revised base flood elevations and update the coastal FIRM panels (FEMA 2012). The mesh covers the counties from Brevard to Martin in central Florida. The resolution varies from 30–50 m in the more complex terrain and developed areas to 80–200 m nearshore, and 1–5 km at the offshore boundary (BakerAECOM 2013). The SFL mesh covers the FL counties from Monroe to Palm Beach (BakerAECOM 2016; Bender 2015). Its resolution is the highest of the five component meshes, with an element spacing of approximately 75 m along the Atlantic coastline and the Florida Keys. The resolution goes down to 10–25 m to describe the complex canal systems in Broward County, Florida.

In addition to the five regional meshes, an open-water mesh was developed by removing floodplains from the HSOFS mesh (Riverside Technology and AECOM 2015). To identify the floodplains, the landward boundary along the US coast in the EC2001 mesh (Mukai et al. 2002) and maximum water levels from a 30-day tides-only HSOFS simulation were used as guidelines. This open-water mesh mostly has its boundary along the coastline but also includes large water bodies like Galveston and Trinity Bay in Texas, Lake Pontchartrain and Chandeleur Sound in Louisiana, Mobile Bay in Alabama, Tampa Bay in Florida, Ossabaw Sound in Georgia, Bulls Bay in South Carolina, and Pamlico Sound in North Carolina. It has 616,113 vertices, which is about one-third the total size of the HSOFS mesh.

#### Creation of SAB Mesh

The five regional meshes were merged onto the open-water mesh to create the SAB mesh with high-resolution coverage of the floodplains from FL through NC. Before merging the meshes, the open-water mesh was converted so that its bathymetry and topography were referenced to the North America Vertical Datum of 1988 (NAVD88) (Riverside Technology and AECOM 2015), so that its ground surface elevations are consistent with the regional

**Table 2.** Spatially varying attributes of the various component meshes: the classes for eddy viscosity and Tau0 are also given

| Mesh | Eddy viscosity | Tau0 | ManningsN | z0Land | VCanopy | Geoid offset | Start dry | Initial river elevation |
|---|---|---|---|---|---|---|---|---|
| NC9 | 2, 10 | 0.005, 0.03 | X | X | X | — | — | X |
| SC | — | 0.005, 0.02, 0.03 | X | X | X | — | — | — |
| GANEFL | 5, 10, 20 | 0.02, 0.03 | X | X | X | X | — | — |
| ECCFL | 10, 20 | 0.02, 0.03 | X | X | X | X | — | — |
| SFL | — | 0.005, 0.02, 0.03 | X | X | X | X | — | — |
| HSOFS | — | 0.005, 0.02, 0.03 | X | X | X | — | X | — |
| SAB | 20, 50 | 0.005, 0.02, 0.03 | X | X | X | — | — | — |

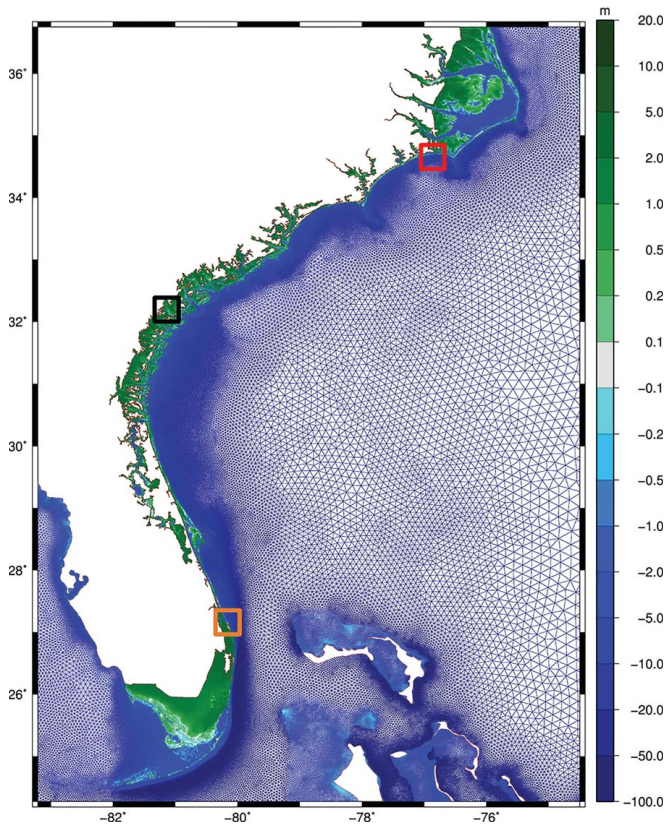


**Fig. 1.** SAB mesh bathymetry and topography (m relative to NAVD88) contoured on the mesh elements. Boxes indicate specific regions, as shown in Fig. 3.

meshes. In addition, regions with ground surface elevations higher than 5 m, which are not likely to be flooded for most storms in this region, were removed from the regional meshes.

Then, decisions were made regarding where the regional meshes merge onto the open-water mesh, what to do at overlapping boundaries between regional meshes, and how to deal with resolution differences at merging boundaries. The regional meshes were merged into the open-water mesh at the 30 m bathymetric contour. This was done to prevent any misalignment in bathymetric and topographic features between the regional and open-water mesh, close to the coastline. At the intermesh boundaries, the regional mesh with higher representation of the topography and bathymetry was used. For differences in resolution at the intermesh boundaries and at the boundaries between the regional and open-water mesh, buffers were created to allow smooth transitions in element spacing. The widths of these buffers thus depends on the resolution differences between the regional meshes and the open-water mesh.

In addition to the ground surface elevations, the SAB mesh also required assignment of the following seven spatially varying attributes: horizontal eddy viscosity, primitive weighting in continuity equation (Tau0), Manning's $n$ at sea floor (ManningsN), surface directional effective roughness length (z0Land), surface canopy coefficient (VCanopy), elemental slope limiter, and advection state. For the eddy viscosity and Tau0, values were defined in classes that were most common among the regional meshes, based on bathymetric depth. For other attributes, values were mapped from the regional meshes wherever possible, or from the HSOFS mesh at locations where that attribute was missing in the corresponding regional mesh. Attributes for elemental slope limiter and advection state were added to stabilize the model. Table 2 gives the attributes present in the component meshes. Details regarding each of the attributes are given in Thomas (2020).

## Comparison with HSOFS Mesh

The SAB mesh was created with an aim of providing detailed coverage of the floodplains from FL to NC (Fig. 1). It has a total of 5,584,241 vertices and 11,066,018 elements. Thus, it is roughly three times the size of the HSOFS mesh, which was developed to provide widespread coverage of floodplains all along the entire US coast, so that its average coastal resolution was limited to 500 m. In contrast, the SAB mesh has an element spacing of less than 100 m along the southeastern US coastline, except in a few regions along the South and North Carolina coasts (Fig. 2). The element sizes are smaller than 20 m in some inland regions.

The advantage of this higher resolution in the SAB mesh can be highlighted at three locations along the US southeast coast, each representing a different type of coastal feature (Fig. 3). At the Saint Lucie Inlet in Florida [Figs. 3(e and f)], the SAB mesh has a resolution of 50 to 100 m. The narrow inlet and channels that travel inland from the shoreline are resolved to accommodate the large flows that need to be transferred to the surrounding marshes and bays. The HSOFS mesh has a resolution of 300 to 500 m, with just one element across the inlet and in some of the adjoining channels. The bathymetry in this region is also represented differently. The inlet has a width of 500 m in the SAB mesh, with a depth of 2.7 m at the center of the inlet. The HSOFS mesh has these values at 640 and 1.3 m, respectively.

Moving north, upstream of the Savannah River along the Georgia–South Carolina border [Figs. 3(c and d)], the SAB mesh has a clear description of the main channel and its tributaries, such as the Little Back River, Middle River, and Wilmington River. These tributaries are absent in the HSOFS mesh, which represents the river at a resolution of 350 to 520 m close to the Sound, and 275 m at the point where it ends upstream. The SAB mesh has an element spacing of about 55 m at the river entrance, and extends about 22 km further inland, as compared with the main channel in the HSOFS mesh. The resolution at the most upstream location of the main channel is 78 m. This higher resolution in the SAB mesh is important in increasing the accuracy for tidal signals, as propagation

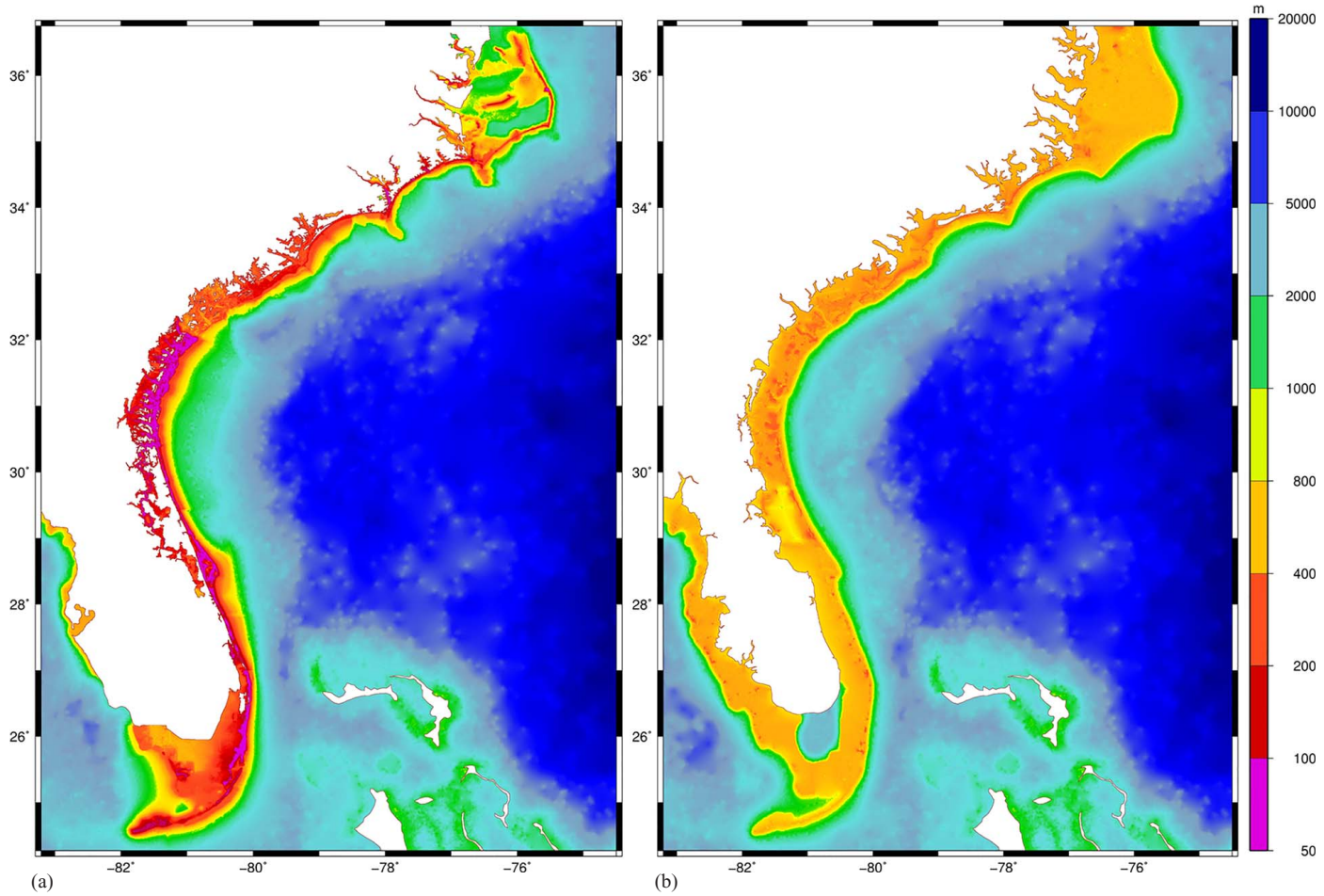


**Fig. 2.** Element spacing (m) along the US southeast coast in (a) SAB mesh; and (b) HSOFS mesh.

through narrow conveyances and attenuation plays an important role in capturing tidal dynamics.

At a section of the Outer Banks in North Carolina located south of the Bogue Sound [Figs. 3(a and b)], the HSOFS mesh has a higher resolution, of 725 m at 13 km offshore, compared with 1.7 km in the SAB mesh. But at the coastline, the SAB mesh transitions to much smaller elements, with a resolution of 120 m at the coastline, 120–165 m in the Outer Banks, and 6–170 m in the Bogue Sound. The HSOFS mesh has a uniform spacing of 425 to 450 m from the shoreline to the end of the Sound. It also has just one element across the Outer Banks at a 500 m resolution. There are also differences in the bathymetry and topography values. In the HSOFS mesh, the Bogue Sound has a depth of 1.4 m everywhere, whereas the depths in the SAB mesh vary from 1.4 m close to the Outer Banks to 4 m near the north boundary of the Sound. Thus, although the SAB mesh has a large number of vertices, compared with the HSOFS mesh, it gives a better representation of the complex bathymetric and topographic features, both nearshore and inland.

### Coupled Models for Nearshore Waves and Circulation

All simulations in this study were conducted using the coupled SWAN +ADCIRC models, which have been validated extensively for coastal flooding during tropical cyclones (Bhaskaran et al. 2013; Hope et al. 2013; Suh et al. 2015; Dietrich et al. 2018). Model settings were the same as in a previous study for Hurricane Matthew on the HSOFS mesh (Thomas et al. 2019). The major difference is the ADCIRC time step. Whereas the HSOFS mesh could be run with a time step of 1 s, this was not possible for the SAB mesh, because of its smaller element spacing, especially in SFL, owing to the Courant–Friedrichs–Lewy (CFL) condition. Therefore, a smaller time step of 0.5 s was used to run the SAB mesh. For simulations on the GANEFL and SC meshes, the time steps were 1 and 2 s, respectively.

For all simulations, the ADCIRC version 52.30.13 was used in explicit mode with the lumped mass matrix form of the generalized wave continuity equation (Tanaka et al. 2011). A depth-dependent quadratic friction law was used to apply bottom drag, with the drag coefficient set by the Manning's $n$ value specified for every vertex (Luettich et al. 1992; Luettich and Westerink 2004). The air–sea momentum exchange was parameterized as a wind drag (Garratt 1977) with an upper limit of $C_D = 0.002$, similar to other studies (Dietrich et al. 2011, 2012). A spatially varying offset surface was also used to account for water level processes on longer time scales, such as steric and local sea level rise (Thomas et al. 2019). SWAN version 41.01 was used. The coupling interval was the same as the SWAN time step of 10 min.

### Storms

The SAB mesh was validated through simulations of two tropical cyclones: Matthew (September to October 2016) and Florence (August to September 2018). Matthew was a Category 5 hurricane that affected much of the US southeast coast and made landfall with Category 1 intensity in South Carolina during October 2016

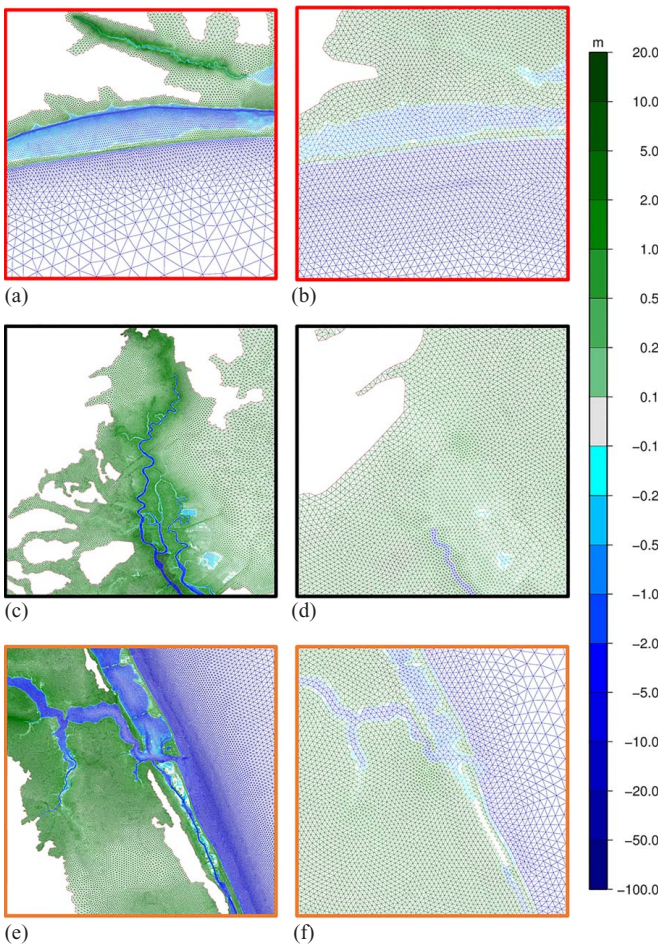


**Fig. 3.** Bathymetry and topography (m) contoured on the mesh elements at locations represented by colored boxes in Fig. 1: (a, c, e) SAB mesh; (b, d, f) HSOFS mesh; (a and b) Outer Banks, NC; (c and d) upstream Savannah River along the Georgia–South Carolina border; and (e and f) Saint Lucie Inlet, FL. The SAB mesh bathymetry is relative to NAV888, whereas the HSOFS mesh values are referenced to local mean sea level (LMSL).

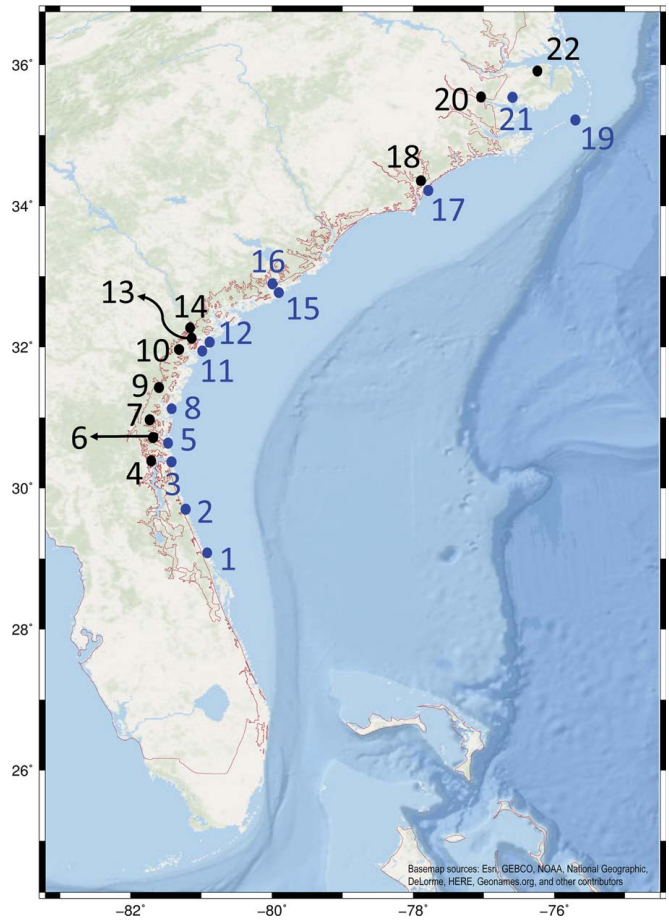


**Fig. 4.** Locations of selected stations for comparison of water levels during Matthew. The stations are numbered from approximately south to north, and the SAB mesh boundary is shown. (Basemap sources: Esri, GEBCO, NOAA, National Geographic, DeLorme, HERE, Geonames.org, and other contributors.)

(Stewart 2017). Florence was a Category 4 hurricane that made landfall in North Carolina during September 2018 (Stewart and Berg 2019) and caused significant storm surge flooding. These two storms were selected because they impacted the US southeast coast where the SAB mesh has detailed coverage. However, whereas Matthew was a shore-parallel storm from FL to NC, Florence had a shore-normal track. They also varied in the size, intensity of winds, duration, and so on.

The storms were represented using data-assimilated wind and pressure fields from Oceanweather Inc. (OWI), as they proved to be the most accurate representation of atmospheric forcing during Hurricane Matthew (Thomas et al. 2019). These atmospheric fields were represented using a lower-resolution basin grid and a higher-resolution regional grid. For Hurricane Matthew, the basin grid covers from 5°N to 47°N and from 99°W to 55°W, with a spatial resolution of 0.25°, whereas the higher-resolution region field covers from 15°N to 40°N and from 82°W to 68°W, with a spatial resolution of 0.05°, both covering a period from 0000 UTC 01 October 2016 to 0000 UTC 11 October 2016, at 15 min intervals. For Hurricane Florence, the basin grid covers from 5°N to 47°N and from 99°W to 55°W, with a spatial resolution of 0.25°, whereas the higher-resolution region field covers from 31°N to 37°N and from 82°W to 74°W, with a spatial resolution of 0.05°, both covering a period from 0000 UTC 07 September 2018 to 0000 UTC 18 September 2018, at 15 min intervals.

To evaluate the model performance, we used observations of water levels at gauges throughout the floodplains. For Hurricane Matthew, an existing collection of observations was used to evaluate the predicted results (Thomas et al. 2019). This included time series of water levels at 501 locations and 612 high-water marks (HWMs). For Hurricane Florence, observations were collected at National Ocean Service (NOS) stations (NOAA 2018), US Geological Survey (USGS) permanent (PERM) (US Geological Survey 2020) and rapidly deployed (DEPL) (US Geological Survey 2018) gauges, and storm tide sensors (STSs) (US Geological Survey 2018). Time series of water levels at 151 locations and 168 HWMs were identified within the model extent in North Carolina. For the analyses herein, those observations that did not operate during the peak of the storm or that had freshwater runoff or wave runup were removed. This left a total of 120 time series, including 6 NOS, 6 USGS-PERM, 11 USGS-DEPL, and 97 USGS-STS, and 85 HWMs to describe the water levels during Hurricane Florence. Such error metrics as root-mean-squared error ($E_{\mathrm{RMS}}$), mean normalized bias ($B_{\mathrm{MN}}$), coefficient of determination ($R^2$), and best-fit slope ($m$) were used to compare modeled results with measurement data.

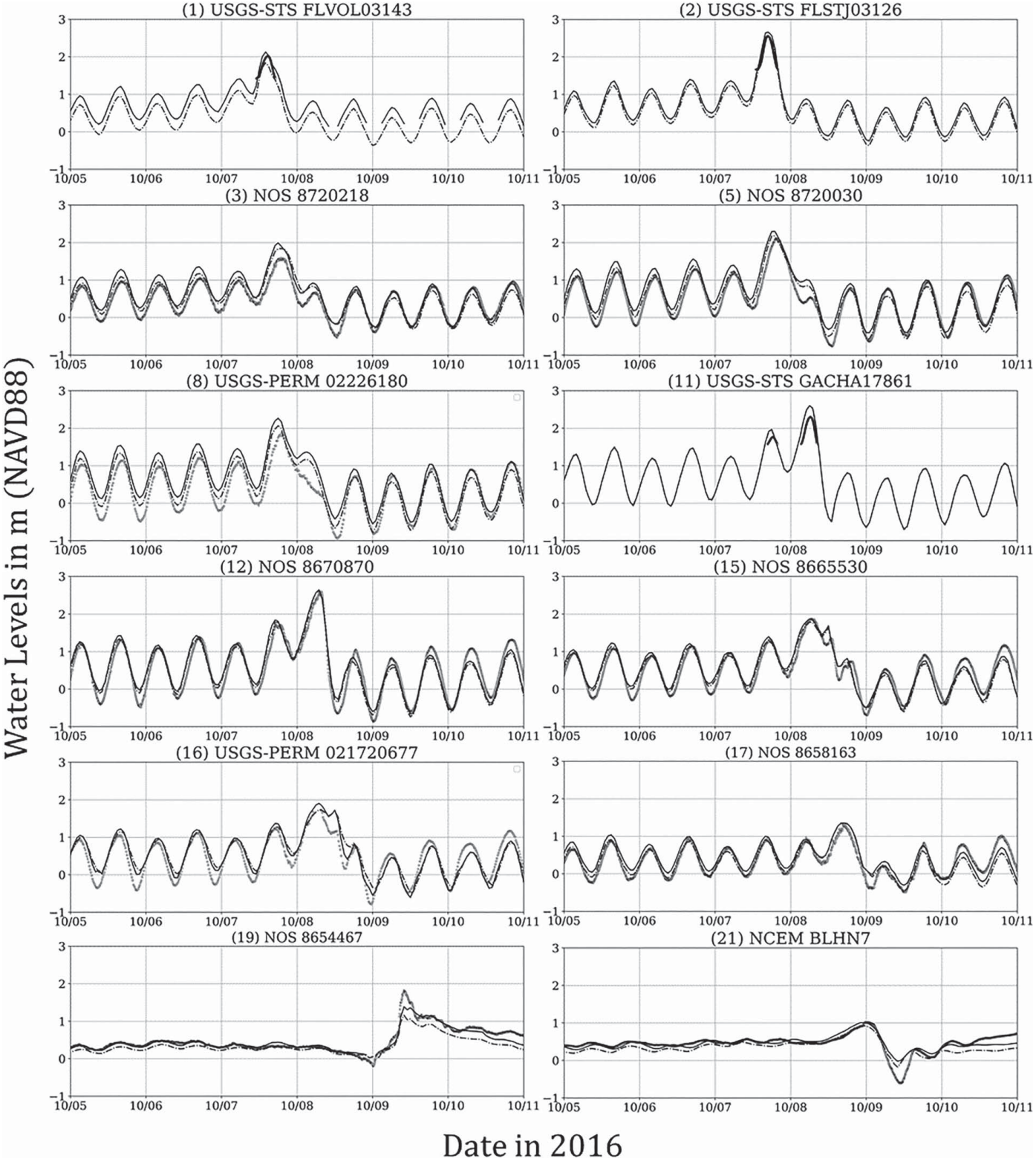


**Fig. 5.** Time series of water levels (m relative to NAVD88) during Hurricane Matthew at the 12 coastal locations shown in Fig. 4. Observed values are shown with gray circles, and predicted results using black lines: (solid) SAB mesh; and (dashed-dotted) HSOFS mesh.

### *Performance*

The wall-clock times for the two simulations were quantified in a previous study (Thomas et al. 2021). On the higher-resolution SAB, for single simulations of Hurricane Matthew (2016) or Hurricane Florence (2018), the wall-clock time was about 43 min per day of simulation. However, when the simulations were "switched" between HSOFS and SAB as the storm approached, the wall-clock times were reduced to averages between 20 and 27 min per day of simulation. These wall-clock timings were obtained using 522 cores on the Stampede2 cluster at the Texas Advanced Computing Center, and they would improve with a higher number of cores (Tanaka et al. 2011). Thus, the SAB mesh can be cost-effective for real-time forecasting.

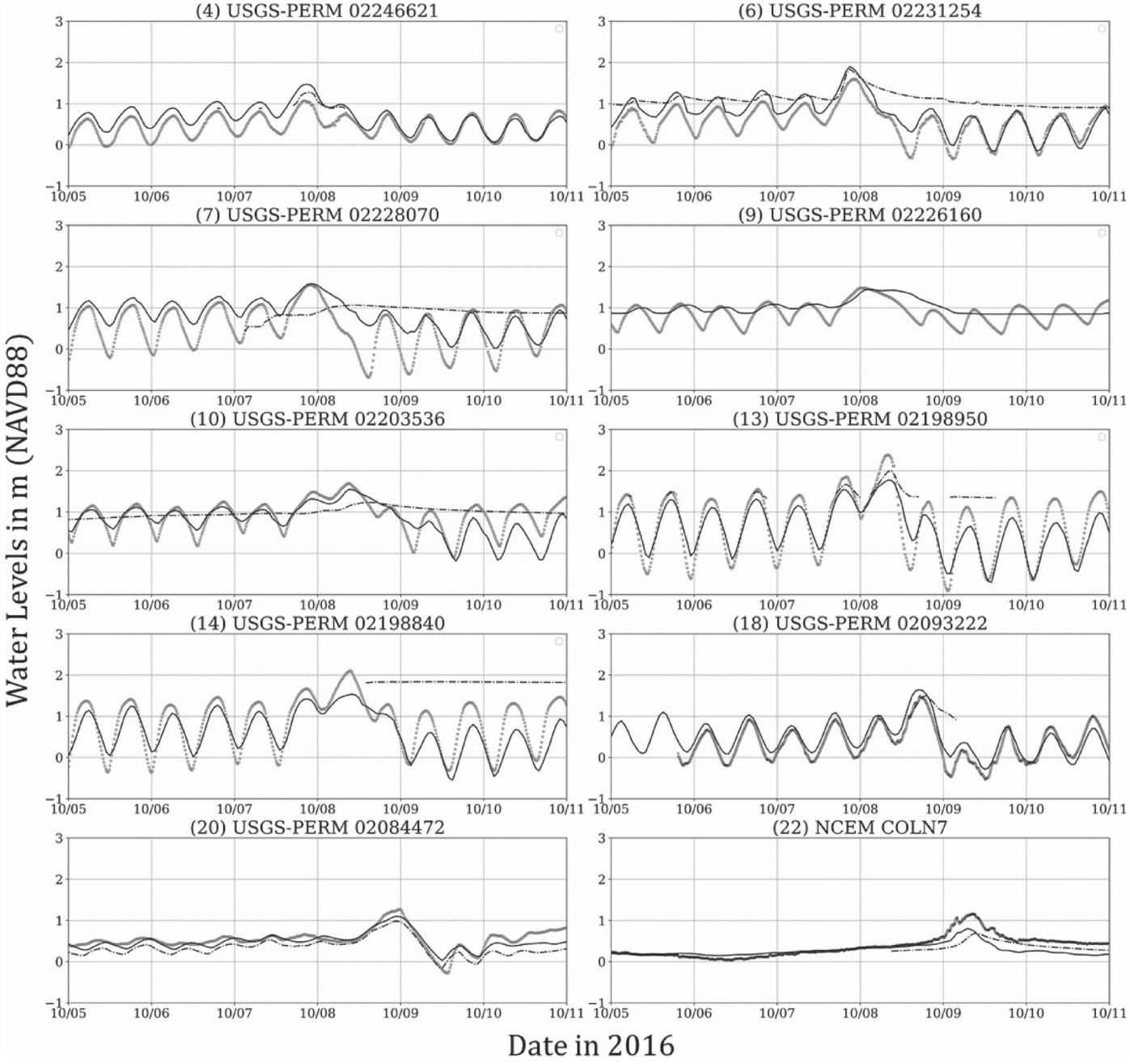


**Fig. 6.** Time series of water levels (m relative to NAVD88) during Hurricane Matthew at the 10 inland locations shown in Fig. 4. Observed values are shown with gray circles, and predicted results using black lines: (solid) SAB mesh; and (dashed-dotted) HSOFS mesh.

## Results and Discussion

### *Hurricane Matthew (2016)*

Water levels were first analyzed by looking at time series plots at 12 locations close to the shoreline, or in the Pamlico Sound in North Carolina (as for the BLHN7 gauge at Belhaven, North Carolina) (Fig. 4), where the HSOFS mesh has adequate resolution to represent bathymetry and topography. Thus, the predicted results using the SAB mesh are similar to results using the HSOFS mesh (Fig. 5). The only noticeable differences are at stations USGS-STS FLVOL03143 and NOS 8654467. At the USGS-STS FLVOL03143 station, located between Orlando Beach and St. Augustine Beach, Florida, the observations indicate a peak of 2.02 m. Although the station remains dry during low tide after the storm peak has passed, the predictions on the SAB mesh are a better match to the observed peak, with a value of 2.12 m, compared with 1.84 m, as predicted on the HSOFS mesh. At the NOS 8564467 gauge at the US Coast Guard station on Hatteras Island, the observed peak was 1.82 m. In the SAB mesh, the channel that leads to this station is represented by elements of 240 m, whereas the element spacing in this area is 525 m in the HSOFS mesh. This leads to a better predicted peak of 1.42 m, as compared with 1.15 m when using the coarser HSOFS results.

The main differences in resolution between the SAB and HSOFS meshes occur far inland, away from the coastline. The predicted time series of water levels (Fig. 6) were therefore compared at 10 stations from FL to NC (Fig. 4), located in small channels or high in the rivers. At the USGS-PERM 02246621 station, located in the Trout River (a tributary of the St. Johns River), Florida,

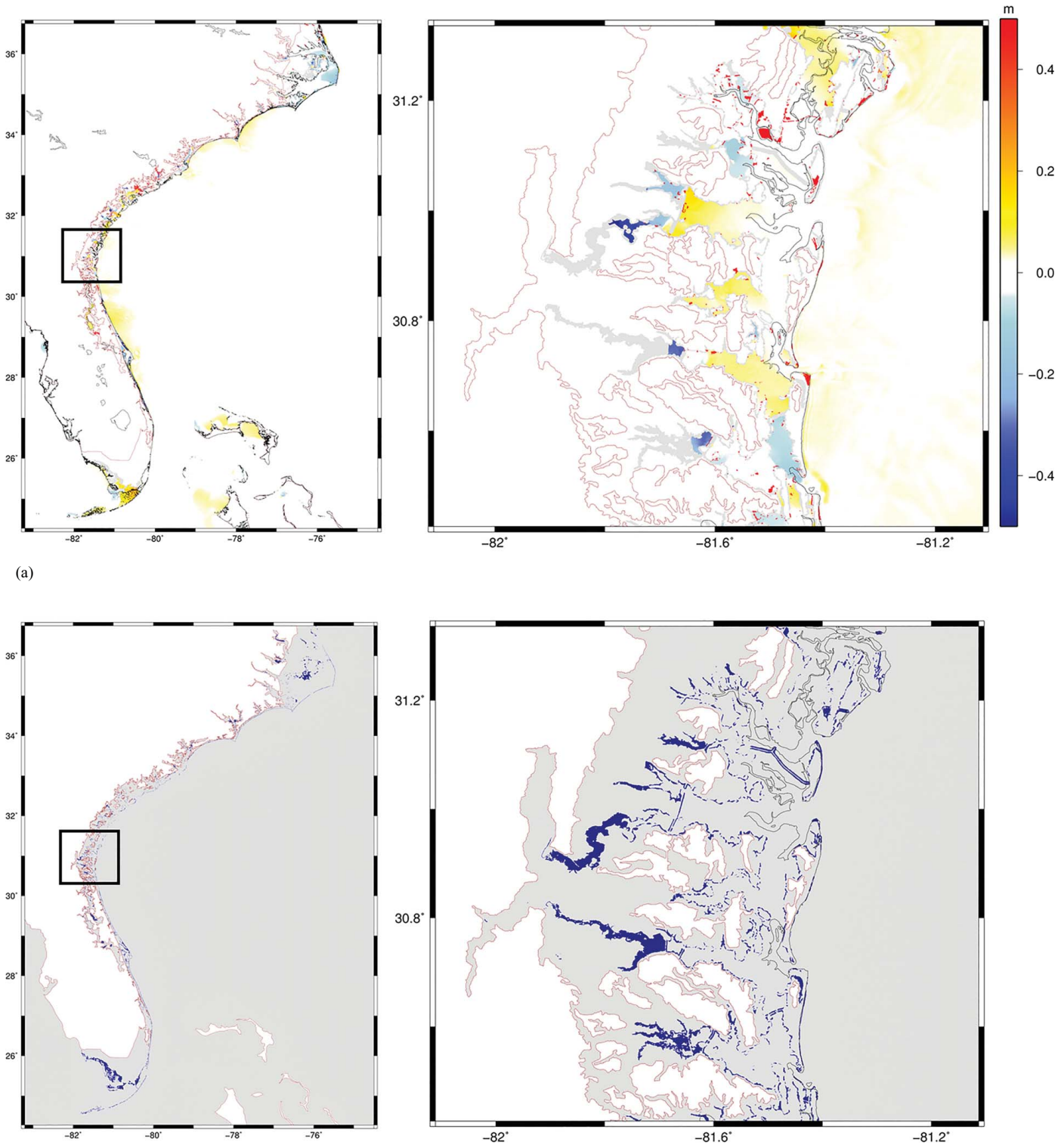


**Fig. 7.** (a) Difference in maximum water levels (m) between the HSOFS and SAB simulations during Matthew. Positive differences indicate increased water levels in the HSOFS mesh simulation, and negative differences indicate increased water levels in the SAB mesh simulation. Locations where the HSOFS mesh was dry but the SAB mesh was wet are indicated without differences. (b) Effect of mesh resolution on inland flooding predictions. Dark regions indicate locations where the HSOFS results were dry and SAB results were wet during Matthew. The box in the left figures indicates the specific region shown on the right. The SAB mesh boundary and coastline are indicated.

the resolution in the channel in the SAB mesh is 44 m. The HSOFS mesh does not resolve this channel, as its element spacing is 280 m in this region, and thus the station remains dry except during the storm peak. The prediction using the SAB mesh does represent the tides and the storm surge, although it overpredicts the peak water levels before and during the storm. At the USGS-PERM 02231254 station, located in the St. Mary's River along the Florida–Georgia border, the trends in the results are the same. The

HSOFS mesh does not have the river extending to this location, owing to its coarser resolution of 342 m. The SAB mesh has the river extending farther inland, with an element spacing of 62 m at the station.

At the USGS-PERM station 02228070, situated in the Satilla River, Georgia, the predictions using the SAB mesh are a good match to the observed peak of 1.5 m. The predictions using the HSOFS mesh indicate a constant value close to 1 m for most of the storm. This inaccurate prediction with the HSOFS mesh is attributed to its poor bathymetry, which has the channel extending to the station location. The resolutions in the SAB and HSOFS meshes at this location are 50 and 379 m, respectively. At the USGS-PERM 02226160 station, located in the Altamaha River, Georgia, the element spacing varies from 60 m in the SAB mesh to 397 m in the HSOFS mesh. This coarser resolution in HSOFS prevents the main river from reaching the station location, and hence the water levels remain dry throughout the simulation. Conversely, although the prediction using the SAB mesh does not capture the tides accurately, it has a good match to the observed peak of 1.48 m, with a value of 1.45 m. The station USGS-PERM 02203536, located in the Ogeechee River, Georgia, is located in an element of size 61 m in the SAB mesh. In the HSOFS mesh, the corresponding element size is 417 m. This is reflected in the predictions using the SAB mesh, which match the observations fairly well, with a good representation of tides and storm surge.

Along the Savannah River on the Georgia–South Carolina border, the HSOFS mesh has a poor representation of bathymetry, owing to its coarser resolution. The USGS-PERM stations 02198840 and 02198950 are located in some of smaller channels in this region. The average resolution at these station locations varies from approximately 52 m in the SAB mesh to 535 m in the HSOFS mesh. The water levels stay dry for most of the simulation using the HSOFS mesh. The SAB results match the observations fairly but underpredict the peak by 0.5 to 0.6 m. At the USGS-PERM 02093222 station, located in the Banks Channel in North Carolina, the SAB mesh results have a good match to the observations although they overpredict the peaks by 0.15 m. The HSOFS results predict only the water levels during the peak of the storm. The channel is absent in the HSOFS mesh, and it has an element spacing of 302 m at this location. The corresponding resolution in the SAB mesh is 155 m.

At the USGS-PERM 02084472 station, located in the Pamlico River, North Carolina, the predictions on both meshes are similar, and match the observations quite well. The SAB mesh results are more accurate, with a better representation of tides before and after the storm. It also has a better match to the observed peak of 1.27 m, with a value of 1.1 m, compared with 0.98 m in the HSOFS mesh results. In this region, the HSOFS mesh has a higher resolution of about 520 m, compared with 760 m in the SAB mesh. At the NCEM COLN7 station, located in the Scuppernong River, which evolves from the Albemarle Sound, the SAB mesh has a resolution of 200 m, compared with a much coarser resolution of 1,300 m in the HSOFS mesh. The observations indicate a maximum water level of 1.15 m at the peak of the storm. The SAB mesh results are a better match in terms of peaks and water levels before the storm. They give a predicted peak of 0.82 m, compared with 0.67 m in the HSOFS results. The HSOFS water levels also remain dry before the storm peak occurs.

### Comparisons of Predicted Flooding Extents

The effects of higher resolution on predictions of overland flooding can be examined by plotting difference maps of maximum water levels between the HSOFS and SAB simulations [Fig. 7(a)]. Differences are shown at the higher resolution by mapping the HSOFS results to the SAB mesh. The values indicate how the maximum water levels at a location in the HSOFS mesh compare with the same location in the SAB mesh.

Overall, there are significant differences between the HSOFS and SAB maximum water levels; these are attributed to the difference in mesh geometry between the two meshes. The differences mainly occur inland, with near-zero differences nearshore and in the open ocean. These differences are in the ranges 0.1 to 0.25 m in the Florida Keys, 0 to 0.3 m in Indian River, Florida, −0.5 to 0.3 m in Savannah River along the Georgia–South Carolina border, and −0.2 to 0.1 m in Pamlico Sound, North Carolina. This is attributed to the higher resolution in the SAB mesh that allows a better representation of bathymetry and, in turn, a better hydraulic connectivity for water to flow into these complex regions. In the HSOFS mesh, the coarser resolution forces the water that cannot flow up into the rivers to pile up, resulting in larger water levels closer to the coast.

The benefit of the added resolution in the SAB mesh is evident at points that were dry during the HSOFS simulation but were wetted in the SAB simulation [Fig. 7(b)], especially in upstream rivers, where the HSOFS mesh does not have sufficient resolution. Thus, the SAB mesh allows for a much larger flooding extent, as compared with the HSOFS results. These trends in the difference in flooding extent between the HSOFS and SAB simulations are supported by the total volume of inundation (Table 4). For an element, this volume is equal to the area of the element multiplied by the average height of water in the three vertices. An element contributes to the total inundation volume only if all the three vertices: (1) have a negative value of $z$ (topography), (2) lie in the affected area of the storm, and (3) were flooded during the simulation. The HSOFS simulation has a much smaller total volume, as it lacks the flooding extent of the SAB simulation.

### Error Statistics

A total of 753 locations were used to evaluate model performance during Hurricane Matthew along the US southeast coast (Thomas et al. 2019). These include the 289 hydrograph-derived peak water levels and 464 USGS-observed HWMs. In Fig. 8, the points are classified based on difference (predicted less observed), expressed as a percentage of observed value. Positive differences indicate overprediction by the model, whereas negative differences indicate underprediction. Out of the 626 stations wetted by ADCIRC, and within the model extent, the errors in the modeled peaks were within 10% at 337 (54%) stations and within 25% at 509 (81%) stations. For the scatter plots, the value of $R^2$ was 0.76 and the slope of the best-fit line was 1.02 (Table 3).

South of Juno Beach in Florida, the model overpredicted the peaks by more than 25%. These regions did not experience storm effects; the total water levels were always less than 1.0 m. It is noted that the SFL and ECCFL component meshes used an initial offset of water levels of −0.155 m and −0.17 m, respectively, but that this attribute was not used with the SAB mesh. The errors were also large on the sound side of the Outer Banks in North Carolina, where the model underpredicted the peaks by more than 25%. The same trends were also seen for the HSOFS simulation (Thomas et al. 2019), although the resolution in the Sound is much higher in the HSOFS mesh (Fig. 2). These larger errors in Pamlico Sound may be caused by inaccuracies in the atmospheric forcing in this region. In other regions, the errors were lesser, especially along the SAB. A positive value of $B_{MN}$ indicated an overprediction of the peaks overall. Although these error statistics are similar to the HSOFS results, the benefit of added resolution in the SAB mesh occurs mainly at inland stations, as seen previously.

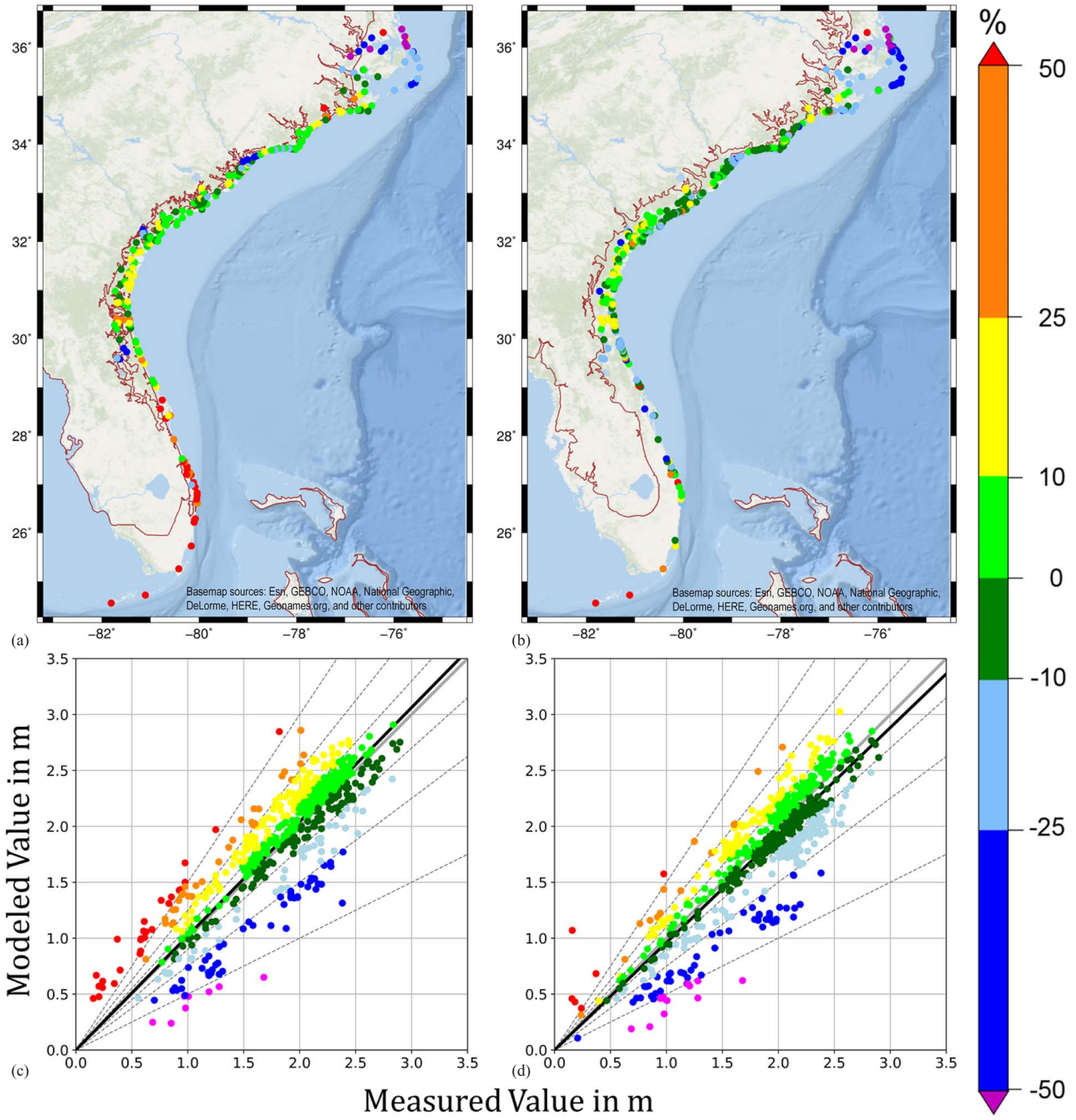


**Fig. 8.** Locations (a and b) and scatter plots (c and d) of HWMs and peak hydrograph values during Matthew: (a and c) SAB; and (b and d) HSOFS. Errors are indicated as a percentage of observed values, and the $y = x$ and best-fit lines are also shown. Statistical metrics are shown in Table 3. (Basemap sources: Esri, GEBCO, NOAA, National Geographic, DeLorme, HERE, Geonames.org, and other contributors.)

### *Hurricane Florence (2018)*

Hurricane Florence was a Category 4 hurricane that made landfall (with Category 1 intensity) along the southeast coast of North Carolina during September 2018. The capability of the SAB mesh in predicting water levels during Hurricane Florence was first evaluated for time series of water levels at 10 locations in North Carolina (Fig. 9) that were impacted by the storm. The HSOFS predictions were also evaluated, to compare how the difference in resolution between the two meshes translates to a difference in storm surge (Fig. 10). At the NOS 8654467 gauge, located in Hatteras on the sound side of the Outer Banks, the resolution in the SAB mesh is 240 m, whereas that in the HSOFS mesh is 464 m. Regardless of these resolution differences, the bathymetry in the area is fairly the same in both meshes; therefore, the predictions of water levels on both meshes are similar. These predictions represent the storm impacts quite well, including the drawdown during the

**Table 3.** Error statistics for the SAB and HSOFS meshes, for both Hurricane Matthew and Hurricane Florence

| | SAB | | HSOFS | |
|---|---|---|---|---|
| Error | Matthew | Florence | Matthew | Florence |
| Wetted stations | 626 | 190 | 622 | 184 |
| Best-fit slope | 1.02 | 1.00 | 0.96 | 0.99 |
| $R^2$ | 0.76 | 0.91 | 0.78 | 0.91 |
| $E_{RMS}$ (m) | 0.28 | 0.20 | 0.28 | 0.21 |
| $B_{MN}$ | 0.03 | 0.01 | −0.03 | −0.01 |

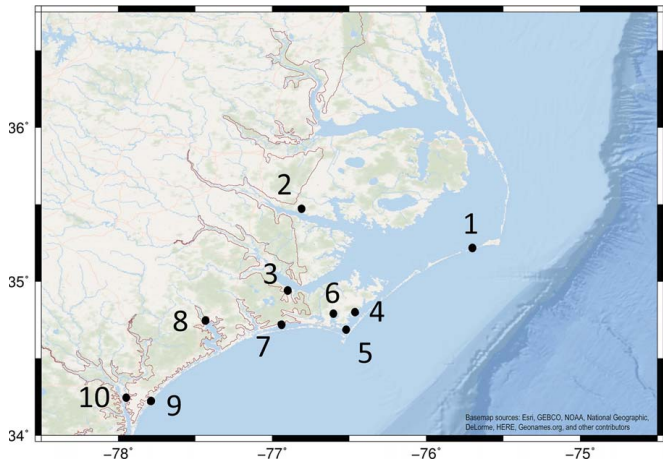


**Fig. 9.** Locations of selected stations for comparison of water levels during Florence. The points are numbered from approximately north to south, and the SAB mesh boundary is shown. (Basemap sources: Esri, GEBCO, NOAA, National Geographic, DeLorme, HERE, Geonames.org, and other contributors.)

storm. The USGS-STS NCBEA11768 gauge, located along Bath Creek, a tributary of the Pamlico River, falls in an element that has an average size of about 1,030 and 380 m in the SAB and HSOFS mesh, respectively. Although the SAB mesh has a much larger element spacing (about three times) in this region, it had a better representation of the channel. In the HSOFS mesh, all three vertices represent topography. Thus, although both meshes had similar predictions during the storm, the SAB mesh captured the tidal effects before the storm peak.

The maximum storm surge inundation heights produced by Hurricane Florence were 2.4 to 3.4 m above ground level along the shores of the Neuse River and its tributaries, where they empty into the Pamlico Sound. Although the Sound has very little tidal influence, the easterly winds from Florence raised water levels on the western side of the Sound and backed up the normal flow of the Neuse River, causing significant shoreline inundation in Craven, Pamlico, and Carteret Counties (Stewart and Berg 2019). The USGS-STS NCCRA13628 gauge, located in Slocum Creek in this area of the Neuse River, observed a peak surge of 3.1 m. For both meshes, the simulations underpredict this observed peak by 0.2 to 0.4 m. The SAB mesh has the channel represented at a resolution of 280 m, whereas it is missing in the HSOFS mesh, with its resolution of 400 m in this region. Thus, the HSOFS predictions do not capture the tidal effects before the storm.

At the USGS-STS NCCAR12128 gauge, located along the Core Sound, the SAB mesh has a resolution of 290 m, whereas that in the HSOFS mesh is about 500 m. The SAB mesh also has a much deeper bathymetry at the center of the Sound, with a value of 3.8 m, compared with 1.6 m in the HSOFS mesh. Although the predictions on both meshes underpredict the peak of the storm, the simulation with the SAB mesh has a better match of 1.45 m to the observed peak of 1.60 m. The corresponding value from the HSOFS mesh is only 1.21 m. At the USGS-STS NCCAR00001 gauge, located on Harkers Island, the simulation with the SAB mesh has a perfect match to the observed peak of 1.2 m, although it slightly over- and underpredicts the water levels before and after the peak. The simulation with the HSOFS mesh underpredicts this peak value by 0.21 m. The resolution in this region is 121 and 422 m in the SAB and HSOFS meshes, respectively.

At the USGS-STS NCCAR00012 gauge, located up the North River that originates from the Back Sound, the SAB mesh has a resolution of 210 m, compared with 380 m in the HSOFS mesh. Although the predictions from both meshes are similar, the SAB mesh has a much better match to the observed peak value of 1.78 m, with a predicted value of 1.86 m. The simulation with the HSOFS mesh underpredicts the peak by more than 20 cm. The USGS-STS NCCAR12410 gauge is located along the Broad Creek that originates from the Bogue Sound. This small channel is not represented well in either mesh; the HSOFS simulation stays dry at this location, but the SAB mesh is able to record the peak of the storm, with a predicted value of 1.78 m, as compared with the observed peak of 1.96 m.

At the USGS-DEPL 0209303201 gauge, located along the New River in Jacksonville, Florida, the resolution in the SAB mesh is 57 m. The HSOFS mesh, however, has this region represented at 395 m resolution, with the New River ending 2 km south of the station. It therefore stays dry for most of the storm duration, except during the peak. The simulation with the SAB mesh overpredicts the water levels by 0.2 to 0.45 m throughout the storm, including at the peak, where it overpredicts the maximum water levels by 0.42 m. The simulation with the HSOFS mesh overpredicts the observed peak value of 1.58 m by only 0.18 m. After the peak of the storm, both meshes predict similar water levels, although the observations indicate effects of river runoff. At the USGS-DEPL 02093222 gauge, along the Banks Channel, the trends in predicted water levels are similar. The simulation with the HSOFS mesh stays dry for the entire storm duration, except at the peak, with both meshes underpredicting the observed peak value of 2.02 m. The simulation with the SAB mesh also has a better peak prediction of 1.84 m, compared with 1.75 m in the HSOFS results. The HSOFS mesh has a coarser resolution of about 300 m, with this region indicated as topography. The SAB mesh has a smaller element spacing of about 150 m with a proper presentation of the channel.

At the USGS-DEPL 0210869230 gauge, located high up in the Cape Fear River, the SAB mesh has a resolution of 60 m with a bathymetry of about 10 m at the center of the channel. The HSOFS mesh has a much coarser resolution of 330 m, with the channel being only 1.4 m deep. The SAB mesh also has seven elements across the channel, compared with just one element in the HSOFS mesh. These differences in resolution and bathymetry are reflected in the predicted results as well. The SAB mesh results are a better match to water levels before the storm, in terms of both timing and magnitude of the peaks. They also give a better prediction of water levels during the storm, with a predicted peak value of 1.64 m, compared with 1.68 m in the observations.

### Comparisons of Predicted Flooding Extents

Difference maps of maximum water levels between the HSOFS and SAB meshes were plotted to examine the effects of added resolution in the SAB mesh on predictions of flooding [Fig. 11(a)]. As compared with the HSOFS results, the SAB water levels are higher in such regions as the Albemarle Sound, Atlantic Intracoastal

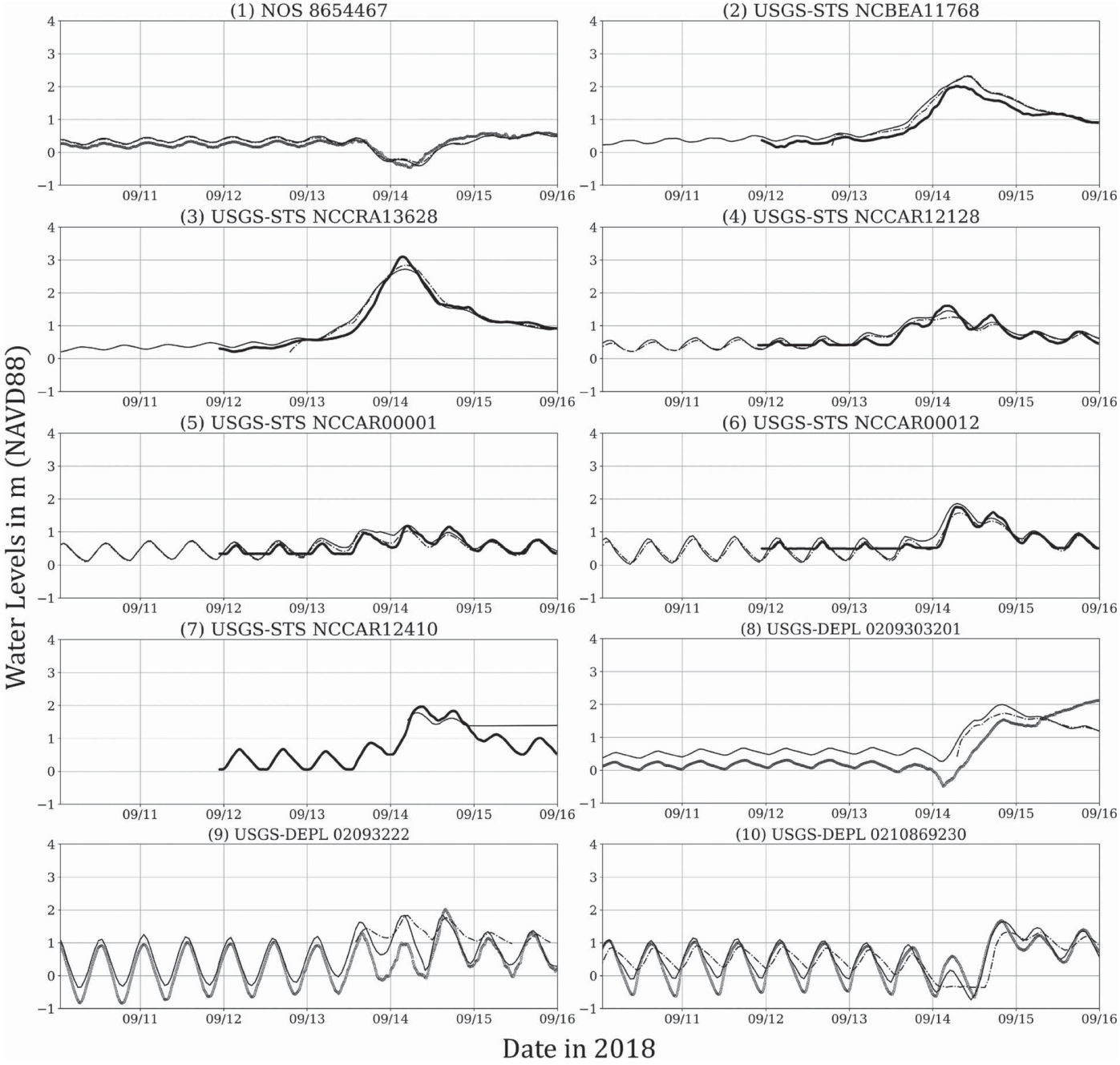


**Fig. 10.** Time series of water levels (m relative to NAVD88) during Hurricane Florence at the 10 locations shown in Fig. 9. Observed values are shown with gray circles, and predicted results using black lines: (solid) SAB mesh; and (dashed-dotted) HSOFS mesh.

Waterway, Core Sound, Currituck Sound, and upstream of all major rivers. These differences were 0.1 to 0.2 m in the Core Sound, 0.2 to 0.6 m upstream of the Neuse River, 0.1 to 0.2 m in the Currituck Sound, and 0.2 to 1 m upstream of the Pamlico River. This is attributed to the higher resolution in the SAB mesh, which better represents the bathymetry, and, in turn, a better hydraulic connectivity for water to flow into these complex regions.

In the HSOFS mesh, the water is not able to flow into the rivers and instead is stuck at downstream locations. Downstream of the Neuse River, the HSOFS water levels were higher by as much as 0.35 m. There are almost zero differences in the open ocean, along the coast, and in the Pamlico Sound. Small differences exist in the northeast region of the domain, far away from the storm's impact. Similar to Hurricane Matthew, the advantage of providing higher resolution is evident at points that were dry during the HSOFS simulation but were wetted in the SAB simulation [Fig. 11(b)]. These additional wetted vertices are located along the wetting–drying regions, such as barrier islands and sounds, as well as upstream of rivers, where the coarser HSOFS mesh does not have sufficient resolution. This larger flooding extent in the SAB mesh is also evident in its higher volume of inundation, as compared with the HSOFS mesh (Table 4).

### Error Statistics

A total of 319 locations were used to evaluate model performance during Hurricane Florence along the North Carolina coast. All stations that were wetted by ADCIRC were included in computing error statistics. Thus, the mesh-to-mesh comparisons may have

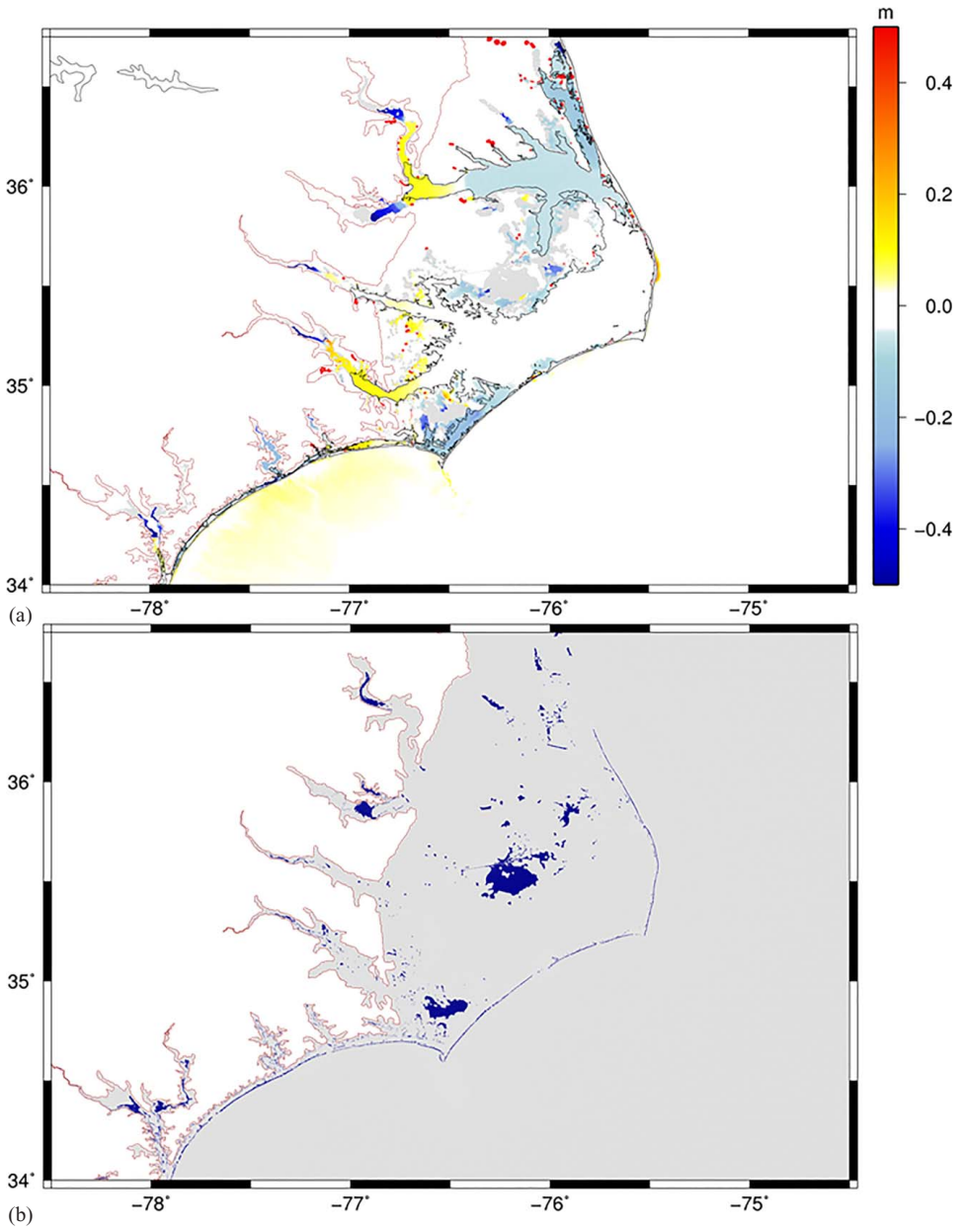


**Fig. 11.** (a) Difference in maximum water levels (m) between the HSOFS and SAB simulations during Florence. (b) Locations where the HSOFS results were dry and SAB results were wet. The SAB mesh boundary and coastline are shown.

**Table 4.** Predicted inundation volumes ($10^9$ $m^3$) for the HSOFS and SAB simulations for Hurricanes Matthew and Florence: the results were mapped onto the SAB mesh, and then inundation volumes were included for elements that (1) had ground surface elevations above mean sea level, (2) were located in the affected area of the storm, and (3) were flooded during the simulation

| | Inundation volume ($10^9$ $m^3$) | |
|---|---|---|
| Storm | HSOFS | SAB |
| Matthew | 3.66 | 5.27 |
| Florence | 0.98 | 1.64 |

different numbers of stations. In Fig. 12, the points are classified based on differences (predicted less observed), expressed as a percentage of observed value. Positive difference indicate overprediction by the model, whereas negative differences indicate underprediction. Out of the 190 locations suitable for peak analysis and wetted by ADCIRC, the errors in the modeled peaks were within 10% at 125 (66%) stations and within 25% at 181 (95%) stations [Figs. 12(a and b)]. For the scatter plots, the value of $R^2$ was 0.91 and the slope of the best-fit line was 1.00 (Table 3). A positive value of $B_{MN}$ indicated an overprediction of the peaks overall. Thus, the ADCIRC prediction on the SAB mesh for Hurricane Florence was a good match to the observations, almost everywhere within the model extent in North Carolina.

A similar analysis was made for the Florence predictions on the HSOFS mesh. Out of the 184 locations wetted by ADCIRC, the errors in the modeled peaks were within 10% at 116 (63%) stations and within 25% at 176 (96%) stations [Figs. 12(c and d)]. For the scatter plots, the value of $R^2$ was 0.91 and the slope of the best-fit line was 0.99 (Table 3). A negative value of $B_{MN}$ indicated an underprediction of the peaks overall. Thus, although the error statistics are similar, the SAB results have a better value of best-fit

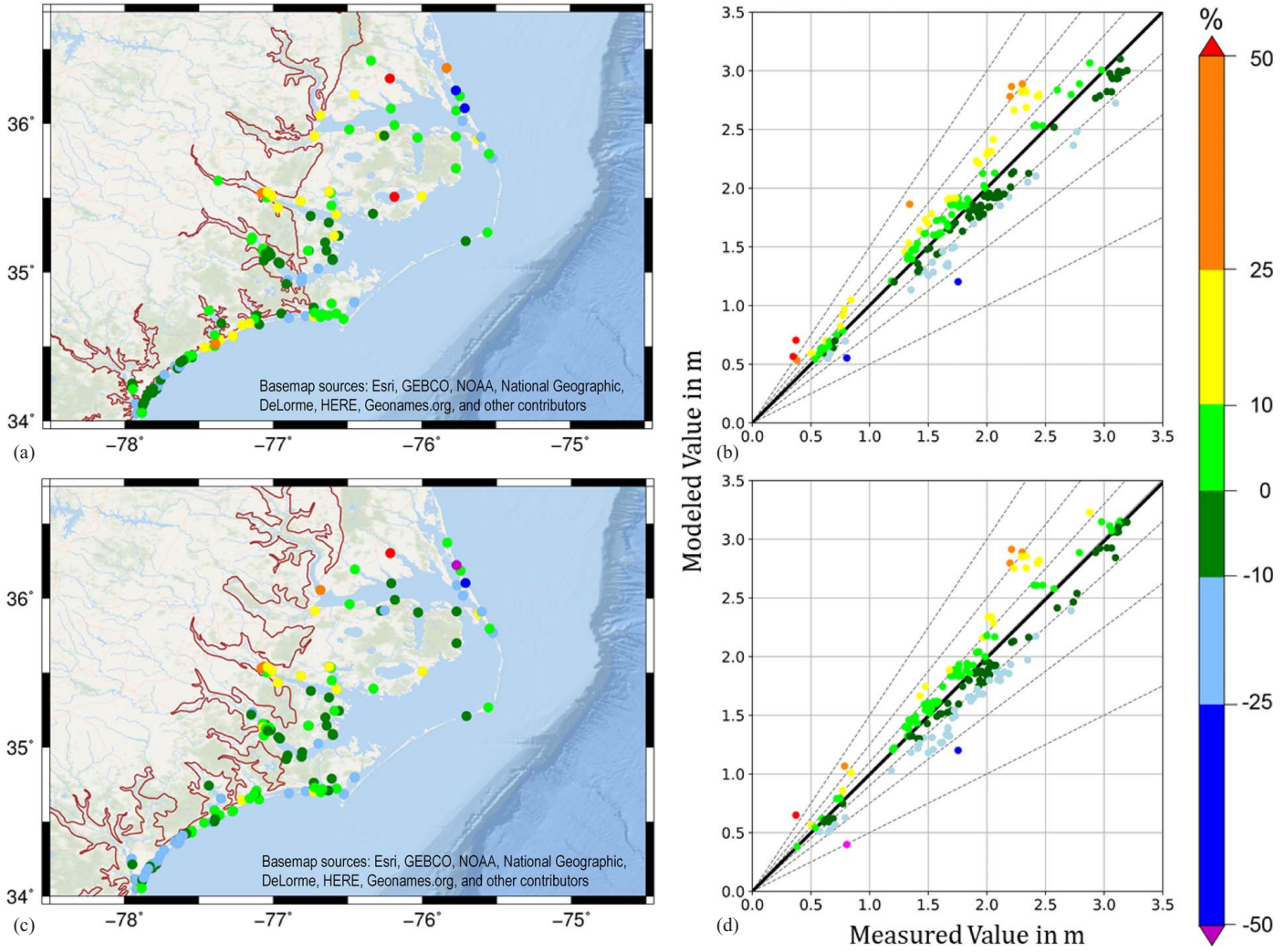


**Fig. 12.** Locations (a and b) and scatter plots (c and d) of HWMs and peak hydrograph values during Florence: (a and c) SAB; and (b and d) HSOFS. Errors are indicated as a percentage of observed values, and the $y = x$ and best-fit lines are also shown. Statistical metrics are shown in Table 3. (Basemap sources: Esri, GEBCO, NOAA, National Geographic, DeLorme, HERE, Geonames.org, and other contributors.)

slope $m$ (closer to 1) and $E_{RMS}$ (closer to 0), and they also flood a large number of stations. These extra stations are located upstream of the major rivers and in the smaller channels, where the HSOFS mesh does not have enough resolution.

### *Benefits of Extended Coverage*

Having quantified the benefits of added resolution in the SAB mesh, we also quantified the benefits of its extended coverage. This was done by comparing predictions of water levels from the SAB mesh during Hurricane Matthew with those from single simulations on the GANEFL and SC meshes. Differences in maximum water levels are shown by mapping the component-mesh results to the SAB mesh as a postprocessing step, so comparisons can be made at the same resolution. As Hurricane Matthew was a shore-parallel storm that moved from south to north along the US southeast coastline, and it had its peak flooding along the Georgia coast, using these two regional meshes will highlight the possible errors associated with using meshes with smaller coverage for flooding predictions.

For the maximum water levels between the GANEFL and SAB meshes [Fig. 13(a)], the differences are close to zero almost everywhere, as the resolutions in the SAB and GANEFL meshes are very similar. Larger differences are seen close to the northern boundary, where the GANEFL mesh overpredicted the flooding by 0.10 to 0.16 m. These boundary effects were visible in the SC mesh predictions as well [Fig. 13(b)]. Along the north boundary of the SC mesh, the maximum water levels were greater than the SAB predictions by 0.1 to 0.25 m. Along the south boundary, the predictions were smaller by 0.1 to 0.26 m. The differences were almost zero in the open ocean. Large differences (greater than 0.5 m) were seen in the floodplains toward the south, as the SC mesh has a much coarser resolution in this region, leading to a poor description of floodplains.

The boundary effects visible in the difference plots of maximum water levels were also seen in the time series plots of water levels at two points located along the north and south boundaries of the GANEFL and SC meshes, respectively [Fig. 13(b)]. At point 1, located close to the north boundary of the GANEFL mesh, the peak water level in the GANEFL results was higher than the SAB mesh maximum water level by 0.15 m. At point 2, located close to the south boundary of the SC mesh, the SC mesh underpredicted the SAB predictions throughout the storm duration. During the storm peak, this difference was 0.25 m. Thus, in addition to providing predictions for a large coastal extent, meshes with large coverage, such as the SAB mesh, can help in avoiding boundary effects associated with smaller-extent regional meshes.

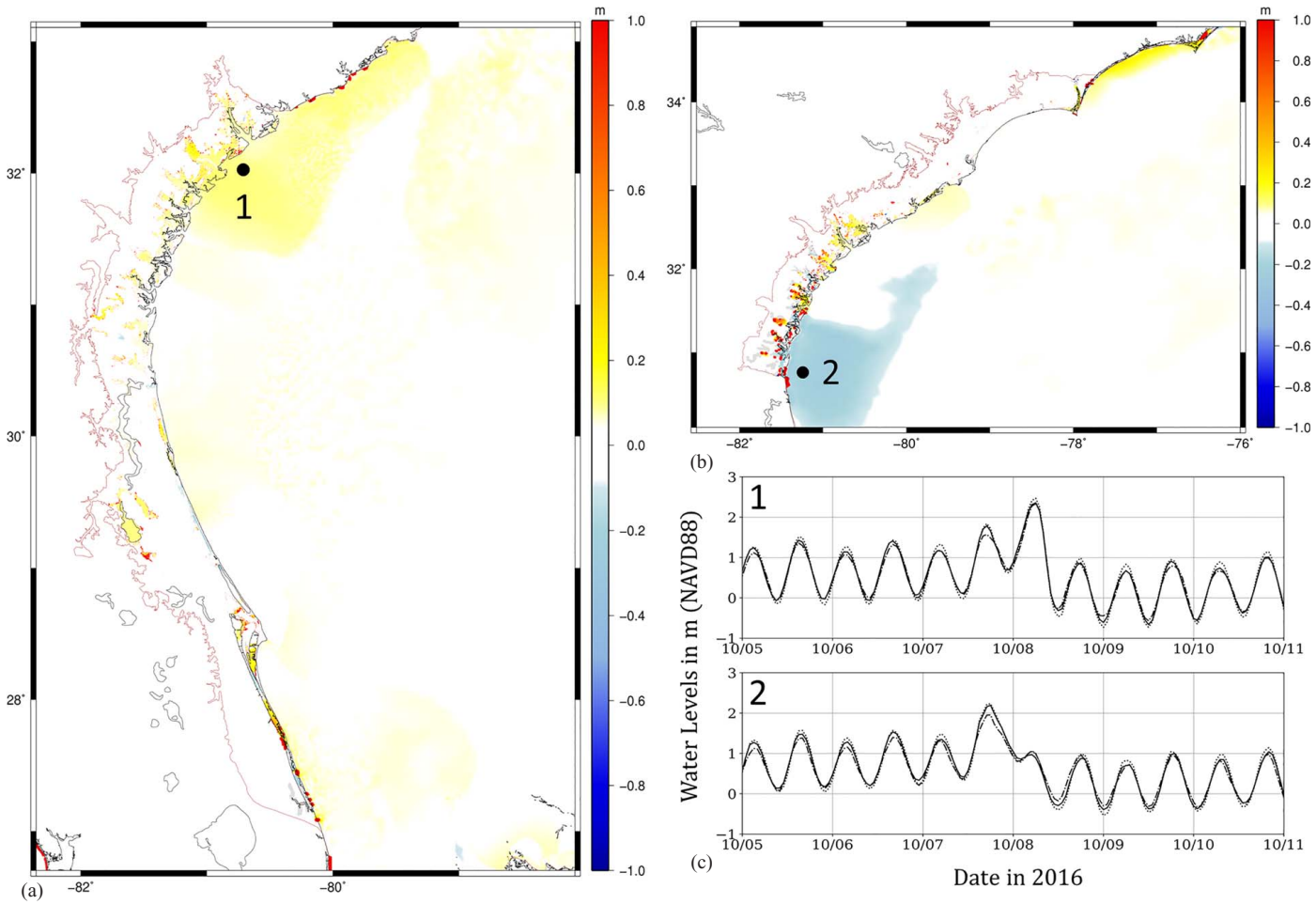


**Fig. 13.** Differences in water levels during simulations of Matthew: (a) difference in maximum water levels between the GANEFL and SAB meshes; (b) difference in maximum water levels between the SC and SAB meshes; and (c) time series of water levels (m relative to NAVD88) at two stations for simulations with: (solid) SAB; (dotted) GANEFL; and (dashed-dotted) SC mesh. The mesh boundaries and coastline are also shown.

## Conclusions

In this study, a high-resolution mesh describing the coastal floodplains from Florida to North Carolina was developed by merging five regional meshes to an open-water mesh. The combined mesh, referred to as the SAB mesh, has 5,584,241 vertices and 11,066,018 elements. The element spacing is less than 100 m along the southeastern US coastline, except in a few regions along the South and North Carolina coasts. The capability of the SAB mesh in accurately predicting flooding was tested by running ADCIRC+SWAN simulations of two storms that impacted the US southeast coast in different ways. The benefits of added resolution in this model were evaluated by comparisons with predictions from a forecast-ready model with a much coarser resolution. The benefits of extended coverage were also quantified by comparing water level predictions from the SAB mesh during Hurricane Matthew with those from single simulations on two regional meshes.

Our findings can be summarized as follows.

1. The new SAB mesh allows predictions of coastal flooding with higher accuracy. For Hurricane Matthew, for 626 locations along the US southeast coast, the SAB mesh had $R^2 = 0.76$, slope of the best-fit line $m = 1.02$, $E_{\mathrm{RMS}} = 0.28$, and $B_{\mathrm{MN}} = 0.03$. For Hurricane Florence, for 120 locations in North Carolina, $R^2 = 0.91$, slope of the best-fit line $m = 1.00$, $E_{\mathrm{RMS}} = 0.20$, and $B_{\mathrm{MN}} = 0.01$. These error statistics for the SAB predictions are either better than or close to those for the HSOFS predictions, meanwhile covering a larger region.
2. Accuracy is improved at inland locations, owing to higher resolution. For both Hurricanes Matthew and Florence, the SAB mesh predicts flooding over a larger region, compared with the corresponding HSOFS simulation. This extra flooding coverage is at such regions as barrier islands or upstream of rivers, where the HSOFS mesh does not have sufficient resolution to provide the required hydraulic connectivity for flooding to occur. The time series of water levels at inland locations indicated that the SAB mesh outperformed the HSOFS mesh in terms of better capturing tidal impacts or having a better match to the peak water levels.
3. Extended coverage is necessary for storms that impact long coastlines. In addition to having a better accuracy of flooding predictions, the SAB mesh, by virtue of its large coverage, eliminates boundary effects associated with smaller regional meshes. Comparisons of water levels during Hurricane Matthew showed that predictions using the GANEFL and SC meshes differed from the SAB predictions by as much as 0.26 m near the mesh boundaries.

It is noted that these findings are specific to the storm surge during the storm's landfall. This study did not consider the rainfall and associated runoff, which affected the region during the days after

the storm made landfall. Future studies will revise the SAB mesh to include upland boundaries, where discharge flow rates can be applied to the coastal rivers. This will enable coupling with hydrologic models to represent compound flooding owing to storm surge and rainfall runoff.

The SAB mesh has been shown to provide accurate predictions of storm surge and coastal flooding for the US southeast coast. Future studies will use the SAB mesh in a new multiresolution approach (Thomas et al. 2021), in which the highest levels of resolution are used only when the storm is expected to cause flooding of coastal regions, especially in forecast applications. Along with other meshes for other regions, e.g., the North Atlantic Coast Comprehensive Study (NACCS) mesh for the northeast US Atlantic coast (Cialone et al. 2017), the system will represent storm-driven flooding along the entire US Gulf and Atlantic coasts. Thus, this study and its findings will contribute to the improvement of real-time forecasts to aid in decision support during landfalling storms.

## Data Availability Statement

The FEMA regional meshes used during the study are available in a repository or online in accordance with funder data retention policies (FEMA 2021). The HSOFS and SAB meshes are available from the corresponding author on reasonable request. ADCIRC is available to researchers on request via its website (https://adcirc.org).

## Acknowledgments

We acknowledge contributions by Chloe Stokes in the processing of the regional meshes. This material is based on work supported by the US Department of Homeland Security under Grant No. 2015-ST-061-ND0001-01. The views and conclusions contained in this document are those of the authors and should not be interpreted as necessarily representing the official policies, either expressed or implied, of the US Department of Homeland Security. This work was also supported by the NSF Grant No. ENH-1635784.

## References

Bacopoulos, P., and S. C. Hagen. 2017. "The intertidal zones of the South Atlantic Bight and their local and regional influence on astronomical tides." *Ocean Modell.* 119: 13–34. https://doi.org/10.1016/j.ocemod.2017.09.002.

BakerAECOM. 2013. *Hydrodynamic and wave model development*. Rep. No. Task Order 114 - East Central Florida Flood Insurance Study.

BakerAECOM. 2016. *Hydrodynamic and wave model development*. Rep. No. ISD1: Section7 - South Florida Flood Insurance Study.

Bender, C. 2013. "Georgia and Northeast Florida coastal storm surge and mapping study." Accessed April 23, 2020. https://fsbpa.com/2013TechPresentations/Bender.pdf.

Bender, C. 2014. "East Coast Central Florida coastal storm surge and mapping study." Accessed April 23, 2020. http://www.floods.org/Files/Conf2014_ppts/E7_Bender.pdf.

Bender, C. 2015. "South Florida coastal storm surge and mapping study." Accessed April 23, 2020. http://www.floods.org/Files/Conf2015_ppts/A7_Bender.pdf.

Bhaskaran, P. K., S. Nayak, S. R. Bonthu, P. L. N. Murthy, and D. Sen. 2013. "Performance and validation of a coupled parallel ADCIRC-SWAN model for THANE cyclone in the Bay of Bengal." *Environ. Fluid Mech.* 13 (6): 601–623. https://doi.org/10.1007/s10652-013-9284-5.

Blain, C. A., J. J. Westerink, and R. A. Luettich. 1998. "Grid convergence studies for the prediction of hurricane storm surge." *Int. J. Numer. Methods Fluids* 26: 369–401. https://doi.org/10.1002/(ISSN)1097-0363.

Blanton, B. O., and R. A. Luettich. 2008. *North Carolina coastal flood analysis system: Model grid generation*. Rep. No. TR-08-05. Chapel Hill, NC: Renaissance Computing Institute.

Blanton, B. O., F. E. Werner, H. E. Seim, R. A. Luettich, D. R. Lynch, K. W. Smith, G. Voulgaris, F. M. Bingham, and F. Way. 2004. "Barotropic tides in the South Atlantic Bight." *J. Geophys. Res.* 109: 1–17. https://doi.org/10.1029/2004JC002455.

Bunya, S., et al. 2010. "A high-resolution coupled riverine flow, tide, wind, wind wave and storm surge model for southern Louisiana and Mississippi: Part I – Model development and validation." *Mon. Weather Rev.* 138 (2): 345–377. https://doi.org/10.1175/2009MWR2906.1.

CERA. 2021. "Coastal emergency risks assessment." Accessed October 6, 2021. https://cera.coastalrisk.live.

Cialone, M. A., A. S. Grzegorzewski, D. J. Mark, M. A. Bryant, and T. C. Massey. 2017. "Coastal-storm model development and water-level validation for the North Atlantic Coast Comprehensive Study." *J. Waterway, Port, Coastal, Ocean Eng.* 143 (5): 04017031. https://doi.org/10.1061/(ASCE)WW.1943-5460.0000408.

Cyriac, R., J. C. Dietrich, J. G. Fleming, B. O. Blanton, C. Kaiser, C. N. Dawson, and R. A. Luettich. 2018. "Variability in coastal flooding predictions due to forecast errors during Hurricane Arthur (2014)." *Coastal Eng.* 137 (2011): 59–78. https://doi.org/10.1016/j.coastaleng.2018.02.008.

Dietrich, J. C., A. Muhammad, M. Curcic, A. Fathi, C. N. Dawson, S. S. Chen, and R. A. Luettich. 2018. "Sensitivity of storm surge predictions to atmospheric forcing during Hurricane Isaac." *J. Waterway, Port, Coastal, Ocean Eng.* 144 (1): 04017035. https://doi.org/10.1061/(ASCE)WW.1943-5460.0000419.

Dietrich, J. C., S. Tanaka, J. J. Westerink, C. N. Dawson, R. A. Luettich, M. Zijlema, L. H. Holthuijsen, J. M. Smith, L. G. Westerink, and H. J. Westerink. 2012. "Performance of the unstructured-mesh, SWAN+ADCIRC model in computing hurricane waves and surge." *J. Sci. Comput.* 52 (2): 468–497. https://doi.org/10.1007/s10915-011-9555-6.

Dietrich, J. C., et al. 2011. "Hurricane Gustav (2008) waves and storm surge: Hindcast, validation and synoptic analysis in southern Louisiana." *Mon. Weather Rev.* 139 (8): 2488–2522. https://doi.org/10.1175/2011MWR3611.1.

FEMA. 2012. *Discovery meeting: East Coast Central Florida (ECCFL) coastal study*. Washington, DC: FEMA.

FEMA. 2021. *Flood risk study engineering library*. Washington, DC: FEMA.

Garratt, J. R. 1977. "Review of drag coefficients over oceans and continents." *Mon. Weather Rev.* 105: 915–929. https://doi.org/10.1175/1520-0493(1977)105<0915:RODCOO>2.0.CO;2.

Hagen, S. C., J. J. Westerink, and R. L. Kolar. 2000. "One-dimensional finite element grids based on a localized truncation error analysis." *Int. J. Numer. Methods Fluids* 32: 241–261. https://doi.org/10.1002/(ISSN)1097-0363.

Hagen, S. C., J. J. Westerink, R. L. Kolar, and O. Horstmann. 2001. "Two-dimensional, unstructured mesh generation for tidal models." *Int. J. Numer. Methods Fluids* 35: 669–686. https://doi.org/10.1002/(ISSN)1097-0363.

Hope, M. E., et al. 2013. "Hindcast and validation of hurricane Ike (2008) waves, forerunner, and storm surge." *J. Geophys. Res.: Oceans* 118 (9): 4424–4460.

Kerr, P. C., R. C. Martyr, A. S. Donahue, M. E. Hope, J. J. Westerink, R. A., Jr. Kennedy, A. B. Luettich, J. C. Dietrich, C. N. Dawson, and H. J. Westerink. 2013. "US IOOS coastal and ocean modeling testbed: Evaluation of tide, wave, and hurricane surge response sensitivities to mesh resolution and friction in the Gulf of Mexico." *J. Geophys. Res.: Oceans* 118: 4633–4661.

Lawler, S., J. Haddad, and C. M. Ferreira. 2016. "Sensitivity considerations and the impact of spatial scaling for storm surge modeling in wetlands of the Mid-Atlantic region." *Ocean Coastal Manage.* 134 (6): 226–238. https://doi.org/10.1016/j.ocecoaman.2016.10.008.

Luettich, R. A., and J. J. Westerink. 1995. "Continental shelf scale convergence studies with a barotropic tidal model." In Vol. 47 of *Coastal and estuarine studies*, edited by D. R. Lynch and A. M. Davies, 349–372. Washington, DC: American Geophysical Union. https://doi.org/10.1029/CE047.

Luettich, R. A., and J. J. Westerink. 2004. "Formulation and numerical implementation of the 2D/3D ADCIRC finite element model version 44.XX." Accessed October 6, 2021. https://adcirc.org/files/2018/11/adcirc_theory_2004_12_08.pdf.

Luettich, R. A., J. J. Westerink, and N. W. Scheffner. 1992. ADCIRC: An advanced three-dimensional circulation model for shelves coasts and estuaries, report 1: Theory and methodology of ADCIRC-2DDI and ADCIRC-3DL. Dredging Research Program Technical Rep. DRP-92-6. Vicksburg, MS: U.S. Army Engineers Waterways Experiment Station.

Mukai, A., J. J. Westerink, R. A. Luettich, and D. J. Mark. 2002. *A tidal constituent database for the Western North Atlantic Ocean, Gulf of Mexico and Caribbean Sea*. Rep. No. ERDC/CHL TR-02-24. Vicksburg, MS: US Army Engineer Research and Development Center.

Naimaster, A., C. Bender, and W. Miller. 2013. "Advanced estimation of coastal storm surge: Application of SWAN+ADCIRC in Georgia/Northeast Florida storm surge study." In *Proc., ATC and SEI Conf. on Advances in Hurricane Engineering*. 607–617. Reston, VA: ASCE. https://doi.org/10.1061/9780784412626.054.

NOAA (National Oceanic and Atmospheric Administration). 2018. "National Ocean Service." Washington, DC: NOAA.

Riverside Technology and AECOM. 2015. *Mesh development, tidal validation, and hindcast skill assessment of an ADCIRC model for the Hurricane Storm Surge Operational Forecast System on the US Gulf-Atlantic Coast*. Rep. Prepared for National Oceanic and Atmospheric Administration. https://doi.org/10.17615/4z19-y130.

Roberts, K. J., J. C. Dietrich, D. Wirasaet, W. J. Pringle, and J. J. Westerink. 2021. "Dynamic load balancing for predictions of storm surge and coastal flooding." *Environ. Modell. Software* 140 (3): 105045. https://doi.org/10.1016/j.envsoft.2021.105045.

Roberts, K. J., W. J. Pringle, and J. J. Westerink. 2019. "On the automatic and a priori design of unstructured mesh resolution for coastal ocean circulation models." *Ocean Modell.* 144 (4): 101509. https://doi.org/10.1016/j.ocemod.2019.101509.

Scheffner, N. W., and F. C. Carson. 2001. *Coast of South Carolina storm surge study*. Rep. No. TR-01-11. Vicksburg, MS: US Army Corps of Engineers.

Stewart, S. R. 2017. Tropical Cyclone Report for Hurricane Matthew, 28 September – 9 October, 2016. University Park, FL: National Hurricane Center.

Stewart, S. R., and R. Berg. 2019. Tropical Cyclone Report for Hurricane Florence, 31 August – 17 September, 2018. University Park, FL: National Hurricane Center.

Suh, S. W., H. Y. Lee, H. J. Kim, and J. G. Fleming. 2015. "An efficient early warning system for typhoon storm surge based on time-varying advisories by coupled ADCIRC and SWAN." *Ocean Dyn.* 65 (5): 617–646. https://doi.org/10.1007/s10236-015-0820-3.

Tanaka, S., S. Bunya, J. J. Westerink, C. N. Dawson, and R. A. Luettich. 2011. "Scalability of an unstructured grid continuous galerkin based hurricane storm surge model." *J. Sci. Comput.* 46 (3): 329–358. https://doi.org/10.1007/s10915-010-9402-1.

Thomas, A. 2020. "Using a multi-resolution approach to improve the accuracy and efficiency of flooding predictions." Ph.D. thesis, Dept. of Civil, Construction, and Environmental Engineering, North Carolina State Univ.

Thomas, A., J. C. Dietrich, T. G. Asher, B. O. Blanton, A. T. Cox, C. N. Dawson, J. G. Fleming, and R. A. Luettich. 2019. "Influence of storm timing and forward speed on tide-surge interactions during Hurricane Matthew." *Ocean Modell.* 137: 1–19. https://doi.org/10.1016/j.ocemod.2019.03.004.

Thomas, A., J. C. Dietrich, M. Loveland, A. Samii, and C. N. Dawson. 2021. "Improving coastal flooding predictions by switching meshes during a simulation." *Ocean Modell.* 164 (8): 101820. https://doi.org/10.1016/j.ocemod.2021.101820.

URS Corporation. 2009. *South Carolina storm surge project deliverable 1: Grid development report*. Rep. No. 1. San Francisco: URS Corporation.

US Geological Survey. 2018. "USGS flood event viewer." Accessed March 10, 2018. https://water.usgs.gov/floods/FEV/.

US Geological Survey. 2020. "USGS current water data for the nation." Accessed May 23, 2020. https://waterdata.usgs.gov/nwis/rt.

WEC (Water Environment Consultants). 2016. *Phase II storm surge analysis: Post 45 project*. Charleston, SC: WEC.

Westerink, J. J., R. A., Jr. Feyen, J. C. Luettich, J. H. Atkinson, C. N. Dawson, H. J. Roberts, M. D. Powell, J. P. Dunion, E. J. Kubatko, and H. Pourtaheri. 2008. "A basin to channel scale unstructured grid hurricane storm surge model applied to southern Louisiana." *Mon. Weather Rev.* 136 (3): 833–864. https://doi.org/10.1175/2007MWR1946.1.

Westerink, J. J., R. A. Luettich, and N. W. Scheffner. 1993. *ADCIRC: An advanced three-dimensional circulation model for shelves coasts and estuaries, Report 3: Development of a tidal constituent database for the Western North Atlantic and Gulf of Mexico*. Rep. No. DRP-92-6. Vicksburg, MS: US Army Corps of Engineers.

Westerink, J. J., J. C. Muccino, and R. A. Luettich. 1992. "Resolution requirements for a tidal model of the Western North Atlantic and Gulf of Mexico." In *Computational Methods in Water Resources IX*. Vol. 2 of *Mathematical Modeling in Water Resources*, edited by T. F. Russell, 669–674. Southampton, UK: Computational Mechanics Publications.